Development of a Calibration Standard for Spherical Aberration

David C. Compertore, Filipp V. Ignatovich, Matthew E. Herbrand, Michael A. Marcus,

Lumetrics, Inc. 1565 Jefferson Road, Rochester, NY (United States)

ABSTRACT

There are no calibration standards currently available for metrology equipment used to measure spherical aberration. We have selected a set of plano-convex lenses that can be used as spherical aberration calibration standards. The key parameters of the lenses were measured using a nodal optical bench and a low coherence interferometer. Spherical aberrations of the lenses were measured using a commercially available aberrometer, the CrystalWave™, based on a Shack-Hartmann wavefront sensor. The lenses were then modeled in optical modeling software, where the spherical curvatures of the lenses were adjusted to match the key parameters. The measured spherical aberrations were then compared to the values provided by the modeling software.

1. INTRODUCTION

1.1 Intraocular Lenses and Spherical Aberration

Anyone making or using imaging optics may at some point run up against spherical aberration (SA). Spherical aberration is often considered an inherent optical flaw and is present to some degree in all imaging systems[1]. In particular, intraocular lens producers have a strong interest in the SA of their lenses. Intraocular lens designers and producers often add SA to their lenses as a feature. For certain intraocular lenses, the manufacturers have made visual performance claims, based on lenses with specific levels of SA. The claims are backed up with clinical data.

1.2 Cataracts, Surgery and Intraocular Lenses

There are two components of the human eye with significant optical power; the cornea, with about 44 D of refractive power, and the accommodating lens, with about 21 D[2]. These two components combine to image the outside world onto our retinas. All adult eyes have some degree of clouding in their natural lens. If this cloudiness progresses to the point where vision is impaired, cataract surgery is used to correct it. During cataract surgery, the cloudy natural lens is pulverized and removed, leaving the capsular bag empty and ready to receive an intraocular lens. The surgeon inserts an intraocular lens through the capsularhexis into the now empty lens bag, filling the space the natural accommodating lens vacated.

1.3 An Intraocular Lens' Multiple Duties

An intraocular lens has many benefits. It returns sight by providing a clean and clear aperture to a once cloudy eye. Of all surgeries performed around the world, cataract surgery is ranked number one for patient satisfaction[3]. Selecting the proper dioptric power for the IOL can correct with great accuracy a person's long standing refractive error, eliminating the need for spectacles for distance vision. In addition, aberrations can be added to the lens, to counterbalance the aberrations present in the patient's cornea, and therefore sharpen the image. It is common for manufacturers to add SA to the intraocular lens, ranging from zero to the amount equal to the opposite of the SA present in the average human cornea. Lenses that contain zero SA, sometimes help to minimize the effects of decentering and tilt inherent in every eye.

A spherical aberration standard lens, as a calibration artifact, will therefore help ensure consistent production quality for intraocular lenses with targeted designed levels of spherical aberration.

1.4 Objectives

The main objective was to create a calibration kit, consisting of a set of lenses with accurately defined amounts of spherical aberration. This set will then be simple to use and understand in the context of SA calibration. The lenses should easily fit into an intraocular lens test bench, and should not exceed in outer diameter the size of a typical intraocular lens, including the haptics, see Figure 1, which help center the intraocular lens in the eye after surgery.

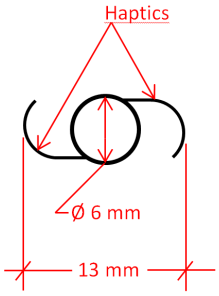

Figure 1: Sample Intraocular Lens

2. Method

2.1 Overview

To minimize the number of lens parameters that can contribute to SA, and therefore to make the SA performance easy to understand, we have selected plano-convex glass lenses. The SA of a plano-convex lens is well documented[4], and a plano-convex lens design is easy to model in any lens modeling software.

We modeled the transmitted spherical aberration of the lenses in Zemax. We then measured the transmitted SA of the lenses using a Shack-Hartmann instrument, the Lumetrics® CrystalWave™. The difference between the modeled spherical aberration and the measured spherical aberration was then compared against the acceptance criterion.

2.2 Modeling

We assume that the convex surface of the lens is perfectly spherical. A generic plano-convex lens is modeled in Zemax. The exact modeling requires the glass material, center thickness of the lens, as well as the radius of curvature of the convex surface.

The center thickness of the lens is measured using the Lumetrics OptiGauge™ low-coherence interferometer. The accurate physical thickness measurement requires the knowledge of the group refractive index of the glass. The OptiGauge™ can also be used to measure the refractive index of the lens material[5]. The measured thickness is then entered into the Zemax model.

The radius of curvature of the lens is found using a Zemax merit function, which adjusts the radius of curvature based on the effective focal length of the lens. The effective focal length of the lenses is measured using an optical nodal bench, a NIST traceable method, by Optical Testing Laboratory, Inc. in Corvallis, OR. Zemax optimizes the curvature of the convex lens surface in the model, until the refined model's effective focal length matches the certified value.

After the model is refined to account for the measured effective focal length and center thickness, four model configurations are set up in the modeling software. By convention, a plano-convex lens has a minimum of spherical

aberration, if the flat surface faces the diverging or converging beam; and maximum SA when it is oriented with the flat surface facing the collimated beam. In creating the certifiable spherical aberration values, we use both orientations of the lens, as well as two different aperture sizes.

The first configuration has a 5 millimeter aperture, with the flat surface of the lens facing the focal point, Figure 2. The second configuration has a 3.6 millimeter aperture, with the flat surface facing the focal point.

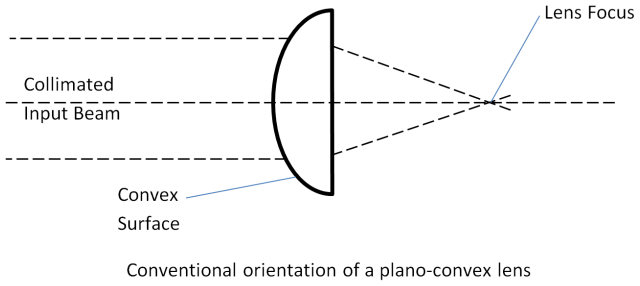

Figure 2: Nominal lens orientation for model configurations 1 and 2.

The lens is flipped around to the non-standard orientation for the third configuration, with a 5 millimeter aperture, Figure 3. The fourth configuration has a 3.6 millimeter aperture, with the convex surface facing the focal point.

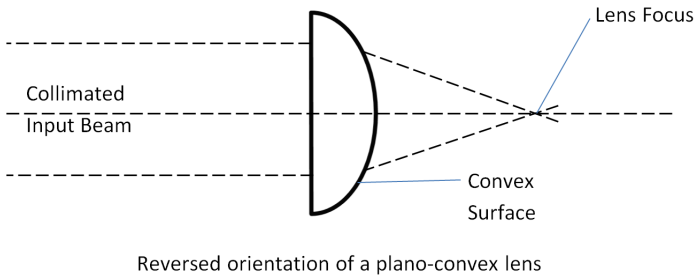

Figure 3: Flipped or reversed orientation for model configurations 3 and 4.

Tables 2, 3, 4 and 5 list the SA values, in the column labeled modeled spherical aberration, obtained using above steps for different lenses and configurations.

2.3 Testing and equipment

Each lens was tested 48 times, 12 times each in four different configurations, on the Shack-Hartmann based instrument. Mechanical fixtures were used to minimize the tip and tilt of the lenses with respect to the measurement beam within the CrystalWave™ instrument. The lenses were centered within the beam by translating the lens about the optic axis to minimize the tilt Zernike terms reported by the Shack-Hartmann. This method works well for lenses that don't have appreciable wedge and will typically center the lenses to within 100 microns on the optic axis. We assumed the lenses had insignificant wedge.

The CrystalWave™ optical configuration is shown in Figure 4. It allows an operator to quickly load and measure intraocular and other types of lenses[6].

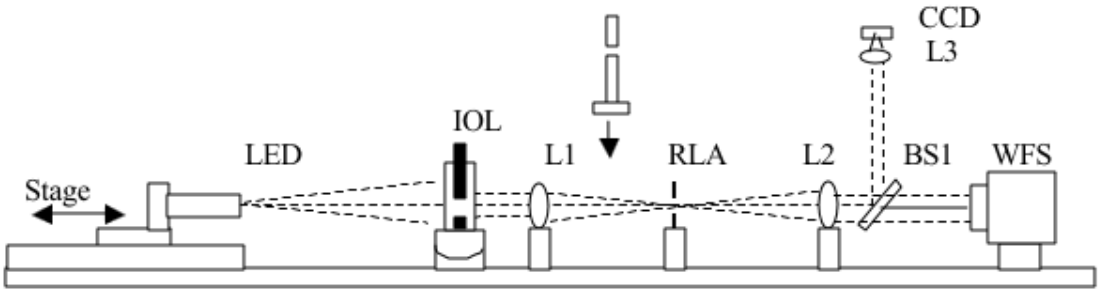

Figure 4: CrystalWave™ optical configuration.

The automated routine moves the point light source, LED in Figure 4, to the position at which the intraocular lens collimates the diverging beam. A collimated input into the Shack-Hartmann sensor, WFS, can be interpreted as an object at infinity, and the point source can be interpreted as light emitted from the retina at the optic axis. Even though the flow of light is reversed compared to the normal function of the eye, the test accurately predicts the optical response of the intraocular lens due to the principle of reciprocity in geometrical optics[7]. The relay lenses, L1 and L2, keep the pupil of the intraocular lens, IOL, conjugate with the lenslet array of the Shack-Hartmann sensor. The rate limiting aperture, RLA, in the relay lens prevents stray light from entering the Shack-Hartmann measurement system.

Each lens is loaded in two different orientations to match those of the Zemax models, in the orientations shown in Figure 2 and 3. The aperture size is controlled by software. A physical aperture was not used to change the aperture size. Two apertures sizes were set in software, 5 mm and 3.6 mm. The two lens orientation and two software-specified apertures result in four total test sets per lens. Each test set contains 12 measurements. After each measurement the lens is shifted from center, rotated, and then centered again. These additional alignment steps are used to average out the operator error due to setup in the measurement values.

2.4 Criteria

The SA measurement value is considered valid for calibration purposes, if the modeled and the averaged measured spherical aberration for the lens are equivalent. A difference of no more than ±0.015 microns of SA between the modeled spherical aberration and the average measured spherical aberration was defined as being equivalent. An absolute difference of 0.015 microns is approximately 3 times smaller than the level of change in spherical aberration a normal eye is able to differentiate[8].

3. Results

Table 1 shows the measured parameter for nine selected of-the-shelf lenses. Each lens has an alphanumeric identification starting with the letters LS, the first column in Table 1. The second column of data contains the manufacturer model number. The third column contains the manufacturer-specified outer diameter of the lenses. The manufacturer-specified effective focal length of the lenses is shown in the fourth column. The fifth column contains the effective focal length, measured by the NIST traceable method. The measured center thickness is listed in the final column.

Table 1: Manufacturer-specified and measured lens parameters.

Lenses ID etched onto the glass	Edmund Optics Model	Diameter (nominal) (mm)	EFL (nominal) (mm)	Certified EFL (mm)	CT measured (mm)
LS-0388	45083	12	12	11.893	4.04319
LS-0389	45083	12	12	11.889	3.99234
LS-0390	45083	12	12	11.896	4.04347
LS-0391	49877	12	20	19.892	3.52611
LS-0392	49877	12	20	19.912	3.52496
LS-0393	49877	12	20	19.904	3.52842
LS-0394	32854	12	60	59.894	2.45257
LS-0395	32854	12	60	59.892	2.46444
LS-0396	32854	12	60	59.951	2.44459

Table 2 shows the modeled and measured SA in the nominal orientations with a 5 mm aperture. Table 3 shows the modeled and measured SA in the reversed orientations with a 5 mm aperture. Table 4 shows the modeled and measured SA in the nominal orientations with a 3.6 mm aperture. Table 5 shows the modeled and measured SA in the reversed orientations with a 3.6 mm aperture. The last column of Tables 2 through 5 tabulates the difference between the measured and modeled SA.

Table 2: The SA, in microns, aperture 5 mm, nominal orientation, modeled in Zemax using parameters from Table 1.

Lenses	modeled Spherical Aberration	Measured Spherical Aberration	Difference (measured - model)
LS-0388	-0.536	-0.540	-0.004
LS-0389	-0.538	-0.540	-0.002
LS-0390	-0.536	-0.537	-0.001
LS-0391	-0.227	-0.222	0.005
LS-0392	-0.226	-0.222	0.004
LS-0393	-0.226	-0.222	0.004
LS-0394	-0.008	-0.003	0.005
LS-0395	-0.008	-0.003	0.005
LS-0396	-0.008	-0.008	0.000

Table 3: The SA, in microns, aperture 5 mm, reversed orientation, modeled in Zemax using parameters from Table 1.

Lenses	modeled Spherical Aberration	Measured Spherical Aberration	Difference (measured - model)
LS-0388	-2.620	-2.723	-0.103

LS-0389	-2.622	-2.717	-0.095
LS-0390	-2.618	-2.713	-0.095
LS-0391	-0.931	-0.937	-0.006
LS-0392	-0.928	-0.931	-0.003
LS-0393	-0.929	-0.933	-0.004
LS-0394	-0.033	-0.027	0.006
LS-0395	-0.033	-0.027	0.006
LS-0396	-0.032	-0.032	0.000

Table 4: The SA, in microns, aperture 3.6 mm, nominal orientation, modeled in Zemax using parameters from Table 1.

Lenses	modeled Spherical Aberration	Measured Spherical Aberration	Difference (measured - model)
LS-0388	-0.142	-0.139	0.003
LS-0389	-0.141	-0.140	0.001
LS-0390	-0.140	-0.137	0.003
LS-0391	-0.060	-0.059	0.001
LS-0392	-0.060	-0.058	0.002
LS-0393	-0.060	-0.058	0.002
LS-0394	-0.002	0.000	0.002
LS-0395	-0.002	-0.003	-0.001
LS-0396	-0.002	-0.004	-0.002

Table 5: The SA, in microns, aperture 3.6 mm, reversed orientation, modeled in Zemax using parameters from Table 1.

Lenses	modeled Spherical Aberration	Measured Spherical Aberration	Difference (measured - model)
LS-0388	-0.685	-0.695	-0.010
LS-0389	-0.686	-0.697	-0.011
LS-0390	-0.685	-0.689	-0.004
LS-0391	-0.244	-0.243	0.001
LS-0392	-0.243	-0.242	0.001
LS-0393	-0.244	-0.242	0.002
LS-0394	-0.009	-0.008	0.001
LS-0395	-0.009	-0.010	-0.001
LS-0396	-0.009	-0.011	-0.002

Figure 5 shows a control limit chart for lens LS-0388. The standard deviation of the 12 measurements is 1 nanometer. The control charts for the other nominally 12 mm EFL lenses are similar.

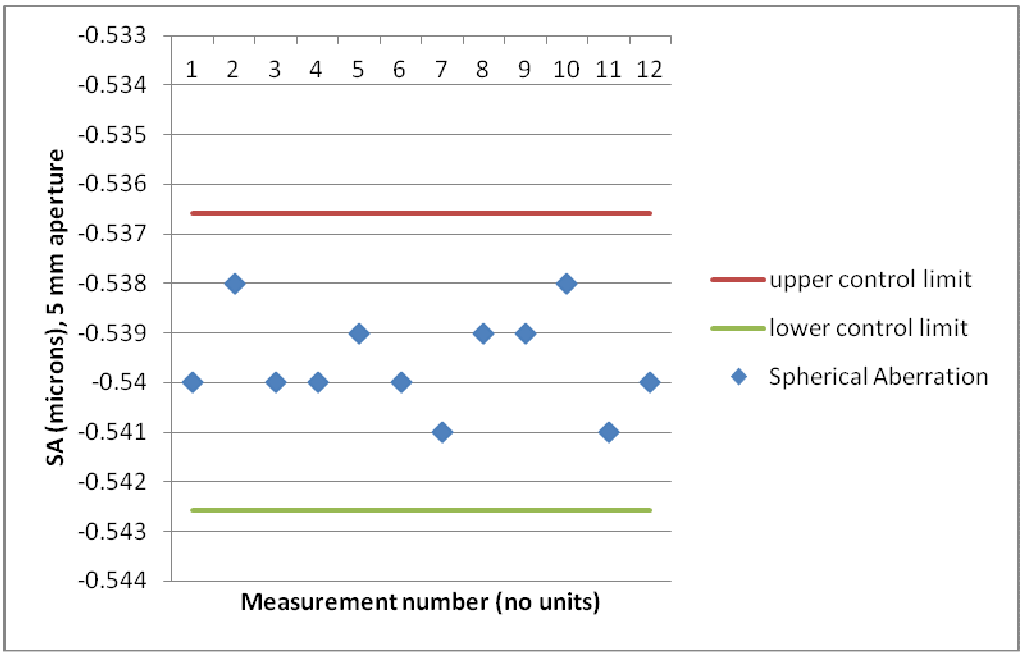

Figure 5: SA control chart for the plano-convex lens LS-0388, nominal orientation, 5 mm aperture.

Figure 6 is a control limit chart for LS-392. The standard deviation of 12 measurements is 3 nanometers.

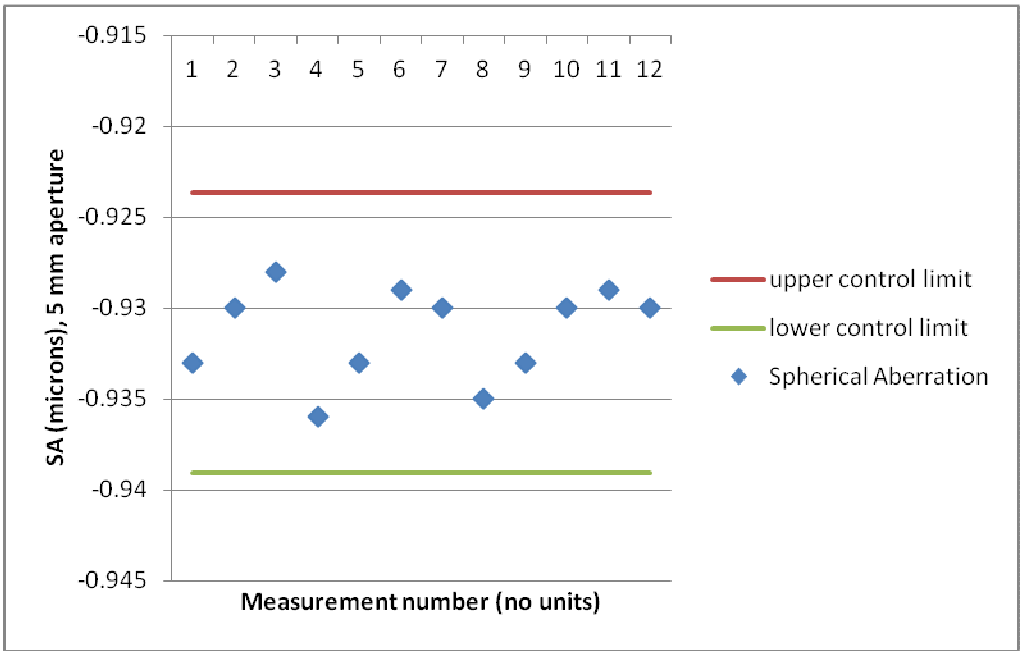

Figure 6: SA control chart for the plano-convex lens LS-0392, reversed orientation, 5 mm aperture

Figure 7 is a control limit chart for lens LS-396. The standard deviation of 12 measurements is 1 nanometer.

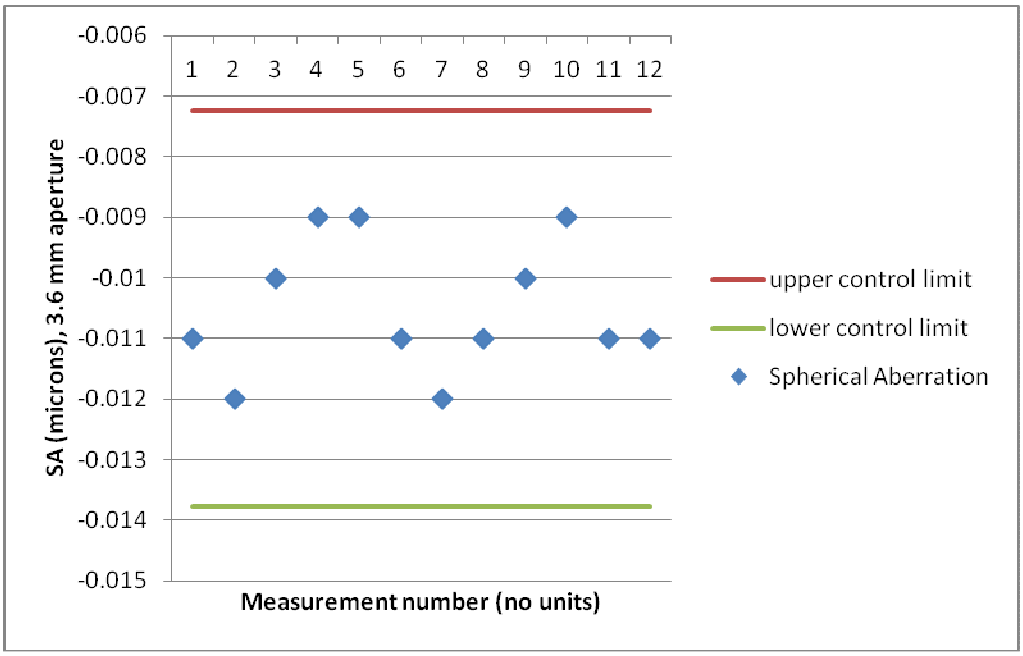

Figure 7: SA control chart for plano-convex lens LS-0396, reversed orientation, 3.6 mm aperture

4. Discussion

4.1 Accuracy or the Agreement between the Model and Measured Results

Figures 5, 6, and 7 are statistical control charts of the spherical aberration measurement process. If all of the measured data falls within the upper and lower control limits the process is considered under control[9]. They show that the process of measuring an intraocular lens is in control. All data points are within the upper or lower control limits for all 36 measurements. We have included only three control charts in this article. Other control charts look similar and the measurements do not cross the control limits.

A summary of the numerical differences, in nm, between the measured and modeled SA for different lenses and configurations are shown in Table 6. Of the 36 spherical aberration tests, 33 configurations pass the acceptance criteria of 0.015 microns or 15 nm.

Table 6: Measured SA minus modeled SA. All numbers are in nm

Lenses	nominal orientation aperture = 5 mm	nominal orientation aperture = 3.6 mm	reversed orientation aperture = 5 mm	reversed orientation aperture = 3.6 mm
LS-0388	-4	3	-103	-10
LS-0389	-2	1	-95	-11
LS-0390	-1	3	-95	-4
LS-0391	5	1	-6	1
LS-0392	4	2	-3	1
LS-0393	4	2	-4	2
LS-0394	5	2	6	1
LS-0395	5	-1	6	-1

LS-0396	0	-2	0	-2

There are three test instances where the acceptance criteria are not met. All three failing instances occurred for the test configuration where the highest spherical aberration was predicted by the model. A review of the Shack-Hartmann test data shows, that in cases with large SA, the Shack-Hartmann operated in out-of-range conditions. Figure 8 shows an example of a Shack-Hartmann area of interest where a neighboring lenslet's spot is infringing, and thus affecting the SA measurement value.

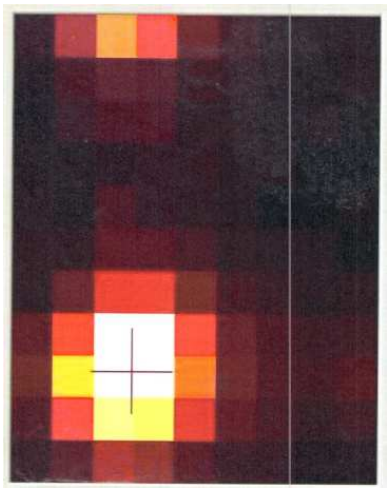

Figure 8: Illustration of the Shack-Hartmann sensor area of interest out-of-range condition, obtained for a configuration with high SA.

This infringing spot comes at the edge of the 5 mm aperture for the 12 mm EFL lens positioned in the reverse orientation, Figure 3. This situation represents an extreme case, as the lens under test is over two times more powerful than the strongest intraocular lens, with its SA nearly an order of magnitude higher than the SA of the average human eye of 0.21 microns over a 5 mm aperture[2]. Care should be taken to maintain SA levels below the levels that can cause out-of-range conditions in the Shack-Hartmann sensor.

4.2 Residual Difference from Modeled to Measured Spherical Aberration

While our results show very good agreement between the modeled spherical aberration and the average measured spherical aberration, there can be two potential sources of error. First source error comes from the assumption that the convex surfaces of the lens are assumed to be perfectly spherical, and the flat surfaces are assumed perfectly flat. It is likely that the spherical surfaces have a small degree of asphericity, and the flat surface is slightly curved. Such deviations contribute to the error in the modeled value of SA. To account for the error, the convex and flat surfaces can be measured in an interferometer, and the measured profile included in the model. Second source of error can stem from the error in the phase index of refraction of the lens, used in the modeling (different from the group refractive index used in thickness measurement). While the above sources of errors are very small, they can have a relatively strong influence on the SA performance of the lens.

5. Conclusion

A simple set of plano-convex glass lenses was successfully calibrated for their spherical aberration. Measuring the lenses in two different orientations provides a useful range of spherical aberration of interest to users of intraocular lens

and intraocular lens manufactures. Users of intraocular lenses and intraocular lens manufactures now have a tool for maintaining the accuracy of their spherical aberration test equipment.

[1] Jenkins, F. and White, H, [Fundamentals of Optics], McGraw-Hill Book Company, New York, pages109-111, (1957).

[2] Liou, Hwey-Lan, Brennan, Noel, A., "Anatomically Accurate, Finite Model Eye for Optical Modeling," J. Opt. Soc. Am. A, Vol. 14, No. 8, pages 1684-1695, (1997).

[3] Steinberg, E.P., Tielsch J.M., Schein O.D., Javitt, J.C., Sharkey, P., Cassard, S.D., Legro, M.W., Diener-West, M., Bass E.B., Daminano, A.M., "National study of cataract surgery outcomes, Variation in 4-month postoperative outcomes as reflected in multiple outcome measures," Ophthalmology, 101 (6), pages 1131-40, (1994).

[4] Sparrold, S., Lansing, A., "Spherical Aberration Compensation Plates," Photonik International, pages 32-35, (2011).

[5] Marcus, Michael, A., Ignatovich, Filipp V., Hadcock, Kyle J., Gibson, Donald S., "Precision interferometric measurements of refractive index of polymers in air and liquid," Optifab, paper 8884-53, (2013).

[6] D. R. Neal, D. J. Armstrong, W.T. Turner, "Wavefront sensor for control and process monitoring in optics manufacture," SPIE 2993, pages 211-220, (1997).

[7] Jenkins, F. and White, H, [Fundamentals of Optics], McGraw-Hill Book Company, New York, page14, (1957).

[8] Legras, Richard, Chateau, Nicholas, Charman, Neil, W., "Assessment of Just-Noticeable Differences for Refractive Errors and Spherical Aberration Using Visual Simulation," OVS, Vol. 81, No. 9, pages 718-728, (2004).

[9] NIST/SEMATECH e-Handbook of Statistical Methods, http://www.itl.nist.gov/div898/handbook/ Section 6.3.1, April 2012